Journal of the Korean Physical Society, Vol. 67, No. 4, August 2015, pp. 663∼667

Surface Plasmon Polaritons of a Symmetric Metamaterial Slab Waveguide with a Hollow Core for Fluid Sensing

Cherl-Hee Lee, Young Ki Cho* and Heung-Sik Tae
School of Electronics Engineering, College of IT Engineering, Kyungpook National University, Daegu 702-701, Korea

YoHan Park
Department of Electronic Engineering, Kyungpook National University, Daegu 702-701, Korea

(Received 5 March 2015, in final form 11 May 2015)

We present a novel waveguide-type fluid sensor with symmetric metamaterial (MTM) slabs by using surface plasmon polaritons (SPP). The presented fluid sensing slabs, consisting of MTM claddings and a hollow core, are designed to have the SPP mode enhance the sensitivity of the fluid sensor. SPP modes are surface waves propagating along the interfaces and decaying exponentially in the transverse direction of the interfaces and are excited in the slabs when a fluid flows into the hollow core, thereby producing evanescent field intensity higher than that of conventional slabs. The eigenvalues of the guiding modes and the SPP mode were graphically derived by using new dispersion equations in a one-dimensional five-layered structure, and the field distributions of the guiding modes and the SPP mode were developed. By designing the refractive indices and widths of the hollow core, the MTM slabs, and the fluid, we can achieve an evanescent field intensity along the interfaces for the presented SPP fluid sensor.

PACS numbers: 41.20.Jb, 41.25.Bs, 42.25.Dd, 84.40.Ba
Keywords: Metamaterials, Surface plasmon polariton, Hollow core, Fluid sensor
DOI: 10.3938/jkps.67.663

I. INTRODUCTION

Recently, metamaterials (MTM), commonly referred to as left-handed materials (LHM), have received considerable attention in the scientific and the engineering communities because of their having simultaneous negative permittivity (ε) and permeability (μ) [1–4]. The MTM-core waveguides have some properties that are different from those of conventional right-handed materials (RHM) waveguides, such as absence of fundamental mode, double degeneracy of modes, and slow propagation sign-varying energy flux [5]. Due to such unusual properties, MTM waveguides have been widely applied to perfect superlenses [6], spatial filters [7], beam shaping [8], and sensors [9–11]. In Refs. [9-11], an optical waveguide using MTM was shown to enhance the evanescent fields of slab waveguides. Because optical waveguide sensors using evanescent waves, such as humidity, bio, chemical, and fluid sensors, generally need evanescent fields strong enough to detect even small changes in evanescent fields to an external stimulus, MTM-waveguide sensors can offer highly effective solutions due to their having enhanced evanescent fields.

A surface polasmon polariton (SPP) is an electromagnetic surface wave travelling along the interface separating a dielectric and a metal. It is produced by the interaction of collective oscillations of free electrons in the metal surface with the electromagnetic wave incident on the metal. SPPs have been widely studied since the anomalous diffraction from a metallic grating was first observed by Wood and Fano [12–14] and have been applied in sub-wavelength optics, data storage, light generation, microscopy, and sensors [15].

Recently, SPP eigenmodes supported at the interfaces between a RHM and a MTM in generalized slab heterostructures were identified and classified by Tsakmakidis *et al.* [16]. Because a SPP is a kind of surface wave that propagates along the interface and decays exponentially in the transverse direction (evanescent), investigations of SPPs propagating along MTM interfaces are beneficial to practical applications owing to their numerous possible applications and unexpected properties. In this paper, we presented a waveguide-type fluid sensor with MTM slabs by using the SPP mode, which improved the amplification of the evanescent waves in the presented structure, leading to enhanced performance of fluid sensing.

*E-mail: ykcho@ee.knu.ac.kr; Fax: +82-53-950-5536

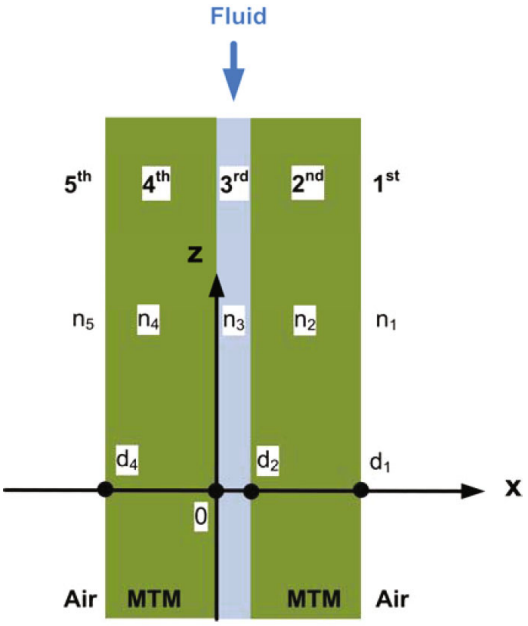

Fig. 1. (Color online) Structure of the presented slab.

II. SPP MODE DESIGN

Figure 1 shows a one-dimensional five-layered slab which is infinite in the y- and z-directions. The slab consists of a first semi-infinite air layer, a second MTM layer with a thickness of (d_1-d_2), a third hollow core layer with a thickness of d_2, a fourth MTM layer with a thickness of d_4, and a fifth semi-infinite air layer. Each layer has a permeability μ_i ($i = 1 \sim 5$), a permittivity ε_i ($i = 1 \sim 5$), and a refractive index n_i ($i = 1 \sim 5$). The hollow core layer with positive permeability μ_3 and permittivity ε_3 is inserted between the MTM layers that are surrounded by air. For simplicity, our investigation was confined to only TE guided modes, $E_y(x)\exp[-j(\beta z - \omega t)]$, where is the angular frequency of the field and ω is the propagation constant in the z-direction.

By using one-dimensional Helmholtz wave equations

$$\frac{\partial^2 E_y}{\partial x^2} + (\omega^2\mu\varepsilon - \beta^2)E_y = 0, \tag{1}$$

the E_y fields at each layer can be described as

$$E_y(x) = \begin{cases} Ae^{-\alpha_1(x-d_1)}, & d_1 \le x, \\ B\cosh[\alpha_2(x-d_2)+\phi_2], & d_2 \le x \le d_1, \\ C\cos(\kappa_3 x) + D\sin(\kappa_3 x), & 0 \le x < d_2, \\ E\cosh[\alpha_4(x+d_4)+\phi_4], & -d_4 \le x \le 0, \\ Fe^{\alpha_5(x+d_4)}, & x \le -d_4, \end{cases} \tag{2}$$

where the transverse wave numbers α_1, α_2, κ_3, α_4, and α_5 correspond to the 1st, 2nd, 3rd, 4th, and 5th layer, respectively, where

$$\begin{aligned} \alpha_1 &= \sqrt{\beta^2 - k_0^2\mu_1\varepsilon_1}, \\ \alpha_2 &= \sqrt{\beta^2 - k_0^2\mu_2\varepsilon_2}, \\ \kappa_3 &= \sqrt{k_0^2\mu_3\varepsilon_3 - \beta^2}, \\ \alpha_4 &= \sqrt{\beta^2 - k_0^2\mu_4\varepsilon_4}, \\ \alpha_5 &= \sqrt{\beta^2 - k_0^2\mu_5\varepsilon_5}. \end{aligned} \tag{3}$$

With the boundary conditions, the tangential component E_y is continuous at $x = d_1$, d_2, 0, and $-d_4$, and the coefficients of E_y are determined as follows:

$$\begin{aligned} A &= \frac{1}{\cos\phi_2}[C\cos(\kappa_3 d_2) + D\sin(\kappa_3 d_2)] \\ &\quad \times \cosh[\alpha_2(d_1 - d_2) + \phi_2], \\ B &= \frac{1}{\cos\phi_2}[C\cos(\kappa_3 d_2) + D\sin(\kappa_3 d_2)], \\ E &= \frac{1}{\cosh[(\alpha_4 d_4) + \phi_4]}C, \\ F &= \frac{\cosh(\phi_4)}{\cosh[(\alpha_4 d_4) + \phi_4]}C. \end{aligned} \tag{4}$$

From Eq. 3, the E_y field at each layer can be given by

$$E_y(x) = \begin{cases} \frac{1}{\cos\phi_2}[C\cos(\kappa_3 d_2) + D\sin(\kappa_3 d_2)]\cosh[\alpha_2(d_1 - d_2) + \phi_2]e^{-\alpha_1(x-d_1)}, & d_1 \le x, \\ \frac{1}{\cos\phi_2}[C\cos(\kappa_3 d_2) + D\sin(\kappa_3 d_2)]\cosh[\alpha_2(x - d_2) + \phi_2], & d_2 \le x \le d_1, \\ C\cos(\kappa_3 x) + D\sin(\kappa_3 x), & 0 \le x < d_2, \\ \frac{1}{\cosh[(\alpha_4 d_4)+\phi_4]}C\cosh[\alpha_4(x + d_4) + \phi_4], & -d_4 \le x \le 0, \\ \frac{\cosh(\phi_4)}{\cosh[(\alpha_4 d_4)+\phi_4]}Ce^{\alpha_5(x+d_4)}, & x \le -d_4. \end{cases} \tag{5}$$

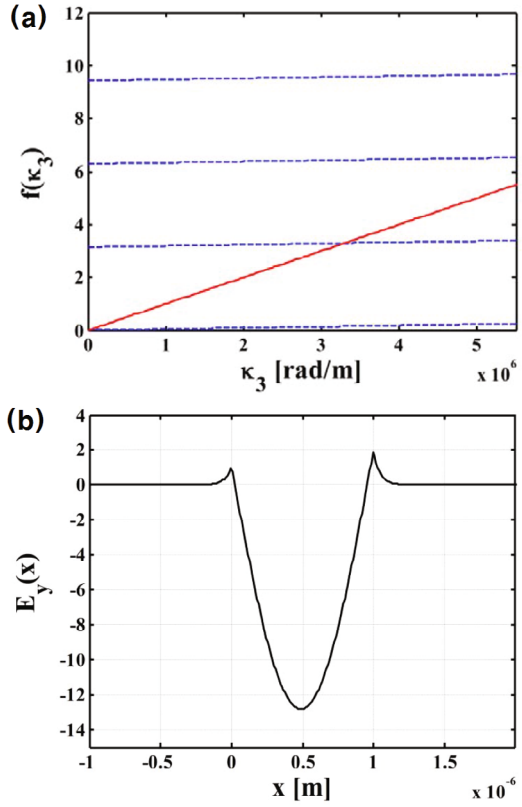

Fig. 2. (Color online) (a) Dispersion curves and (b) field distribution of the symmetric five-layered slab waveguide for the oscillating TE2 guided modes.

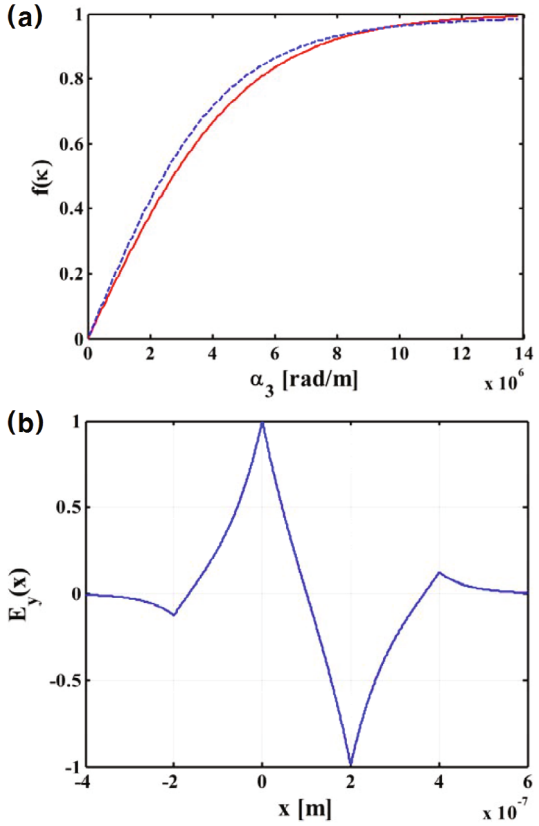

Fig. 3. (Color online) (a) Dispersion curve and (b) field distribution of the presented slab waveguide for the SPP mode.

Using the boundary conditions that the tangential component H_z is continuous at $x = d_1$, d_2, 0, and $-d_4$, we can obtain the following equations:

$$\begin{aligned}
&\frac{1}{\mu_1}(-\alpha_1)A = \frac{1}{\mu_2}\alpha_2 B\sinh[\alpha_2(d_1-d_2)+\phi_2],\\
&\frac{1}{\mu_2}\alpha_2 B\sinh\phi_2 = \frac{1}{\mu_3}[-\kappa_3 C\cos(\kappa_3 d_2)+\kappa_3 D\sin(\kappa_3 d_2)],\\
&\frac{1}{\mu_3}\kappa_3 D = \frac{1}{\mu_4}\alpha_4 E\sinh[\alpha_4 d_4+\phi_4],\\
&\frac{1}{\mu_4}\alpha_4 E\sinh[\alpha_4 d_4+\phi_4] = \frac{1}{\mu_5}\alpha_5 F.
\end{aligned} \tag{6}$$

By substituting Eq. 4 to Eq. 6, the values of ϕ_2, ϕ_4, C, and D are determined as follows:

$$\begin{aligned}
&D = qC,\\
&q = \frac{\mu_3}{\mu_4}\frac{\alpha_4}{\kappa_3}\tanh[(\alpha_4 d_4)+\phi_4],\\
&p = \frac{\mu_3}{\mu_2}\frac{\alpha_2}{\kappa_3},\\
&\tanh(\phi_4) = \frac{\mu_4}{\mu_5}\frac{\alpha_5}{\alpha_4},\\
&\tanh[\alpha_2(d_1-d_2)+\phi_2] = -\frac{\mu_2}{\mu_1}\frac{\alpha_1}{\alpha_2}.
\end{aligned} \tag{7}$$

When κ_3 is real and $k_0^2\mu_3\varepsilon_3 > \beta^2 > k_0^2\mu_2\varepsilon_2 > k_0^2\mu_1\varepsilon_1$, oscillating guided modes can exist in the third RHM-core layer, and we can obtain the dispersion equation of guided modes from Eq. 6 as follows:

$$\tan\kappa_3 d_2 = \frac{q+p(-\tanh\phi_2)}{1-qp(-\tanh\phi_2)}. \tag{8}$$

Equation 8 can be expressed as follows:

$$\kappa_3 d_2 = m\pi + \tan^{-1} q + \tanh^{-1}[-p\tanh(\phi_2)].] \tag{9}$$

Equation 9 is a transcendental equation and cannot be solved analytically; therefore, we use a graphical method to determine κ_3 for the guided modes. After putting the right-hand side of Eq. 9 to f(κ_3), we draw both the left- and the right-hand sides of the equation and find the crossing points of the characteristic curves. The crossing points correspond to eigenvalues for the guided modes.

The left- and the right-hand sides of the characteristic equation, Eq. 5 of a symmetric five-layered slab waveguide are plotted in Fig. 2(a) with red solid and blue dashed lines, which correspond with the mode numbers on the right-hand side of Eq. 9. The crossing points of the characteristic curves in Fig. 2(a) give the eigenvalues of κ_3 while the first-crossing point represents the TE_2 mode. The constitutional parameters were as follows: λ

= 1 μm, ($\mu_1 = 1$, $\varepsilon_1 = 1$), ($\mu_2 = -2$, $\varepsilon_2 = -2$), ($\mu_3 = 4$, $\varepsilon_3 = 4$), ($\mu_4 = -2$, $\varepsilon_4 = -2$), and ($\mu_5 = 1$, $\varepsilon_5 = 1$). The thicknesses of the 2nd and 3rd and 4th layers were 1 μm, 1 μm, and 1 μm, respectively.

Figure 2(b) shows the field distributions of the guided TE_2 mode of the symmetric five-layered RHM slab waveguide. The mode number means the number of intersections between the fields and the x-axis. As the figures show, the electric fields are oscillatory in the RHM-core layer while becoming evanescent outside the MTM-clad layers.

The surface guiding modes, special class of the guided optical modes, exist under certain special conditions at the interface separating two different dielectrics. The negative permittivity and permeability of MTM slabs allow the existence of surface guiding waves at the interfaces with RHM layers. In particular, TE-polarized surface waves exist when the magnetic permeability constants of two dielectric materials have different signs at the interface while TM-polarized surface waves exist when the dielectric permittivity constants of the materials have different signs. In this study, we show the existence of surface waves with TE polarizations in the presented slab waveguide.

When κ_3 is purely imaginary and $\beta^2 > k_0^2\mu_3\varepsilon_3 > k_0^2\mu_2\varepsilon_2 > k_0^2\mu_1\varepsilon_1$, surface modes are guided along the interfaces. Hence, by replacing κ_3 with $i\alpha_3$ in Eq. 8, the dispersion equation for surface guided modes can be obtained as follows:

$$\tanh(\alpha_3 d_2) = -\frac{q + p[-\tanh(\phi_2)]}{1 + qp[-\tanh(\phi_2)]}, \tag{10}$$

where $\alpha_3^2 = \beta^2 - k_0^2\mu_3\varepsilon_3$.

Figure 3 shows that the dispersion curve and the field distribution of the SPP mode, which are calculated by using the characteristic equation, Eq. 10, with the following constitutional parameters: $\lambda = 1$ μm, ($\mu_1 = 1$, $\varepsilon_1 = 1$), ($\mu_2 = -2$, $\varepsilon_2 = -2$), ($\mu_3 = 2.2$, $\varepsilon_3 = 2.2$), ($\mu_4 = -2$, $\varepsilon_4 = -2$), ($\mu_5 = 1$, $\varepsilon_5 = 1$), ($d_1 = 0.2$ μm), and (d_1-$d_2 = 0.2$ μm). In Fig. 3(a), the red dashed and the black solid lines correspond to the right-hand side and the left-hand side of the characteristic equation, Eq. 10, respectively, and the crossing point of the characteristic curves gives the eigenvalue α_3 of the SPP mode. The Poynting vetor, $S_z = \beta E^2(x)/(2\omega\mu)$, is directed along the z-axis, and the directions of energy flux in the MTM layers are opposite to those in the RHM-core layer because of the negative permeability. We can get the net power flux in a slab waveguide by using the normalized power in which the unknown amplitude A of guided modes can be calculated by using the condition ($P_1 + P_2 + P_3 + P_4 + P_5 = 1$W):

$$\begin{aligned}
P_1 &= \frac{1}{4}\frac{\beta}{\omega\mu_1}\frac{A^2}{\alpha_1},\\
P_2 &= \frac{1}{4}\frac{\beta}{\omega\mu_2}B^2\left[(d_1 - d_2) + \frac{1}{2\alpha_2}\{\sinh[2\alpha_2(d_1 - d_2) + 2\phi_2] - \sinh(2\phi_2)\}\right],\\
P_3 &= \frac{1}{4}\frac{\beta}{\omega\mu_3}E^2\left[\left(C^2 d_2 + \frac{CD}{2\kappa_3} + D^2 d_2\right) + \frac{C^2 - D^2}{2\kappa_3}\sin 2\kappa_3 d_2 - \frac{CD}{2\kappa_3}\cos(2\kappa_3 d_2),\right],\\
P_4 &= \frac{1}{4}\frac{\beta}{\omega\mu_4}E^2\left[d_4 + \frac{1}{2\alpha_4}\{\sinh(2\alpha_4 d_4 + 2\phi_4) - \sinh(2\phi_4)\}\right],\\
P_5 &= \frac{1}{4}\frac{\beta}{\omega\mu_F}\frac{F^2}{\alpha_5}.
\end{aligned} \tag{11}$$

III. CONCLUSION

In this paper, a waveguide-type fluid sensor with symmetric metamaterial (MTM) slabs was presented by using surface plasmon polaritons (SPP). The presented fluid-sensing slab waveguide consisted of MTM claddings and a hollow core, and the SPP mode was designed to be excited in the slabs when a fluid flowed into the hollow core, thereby producing an evanescent field intensity higher than that of conventional slabs. The eigenvalue of the SPP was graphically derived by using new dispersion equations in a one-dimensional five-layered structure, and the field distributions of the SPP were developed. If the dimensions of the hollow core and the MTM slabs are designed according to the refractive index of the fluid, the presented SPP fluid sensor can achieve the evanescent field intensity along the interfaces.

ACKNOWLEDGMENTS

This study was supported by BK21 Plus funded by the Ministry of Education, Korea (21A20131600011), and the Basic Science Research Program through the National Research Foundation of Korea (NRF) funded

by the Ministry of Education, Science and Technology (NRF-2010-0024647).

REFERENCES

[1] V. G. Veselago, Soviet Physics Uspekhi **10**, 509 (1968).
[2] D. R. Smith, W. J. Padilla, D. C. Vier, S. C. Nemat-Nasser, S. Schultz, R. A. Shelby, D. R. Smith and S. Schultz, Phys. Rev. Lett. **84**, 4184 (2000).
[3] K. Y. Kim, J-H. Lee, Y. K. Cho and J-H. Lee, Opt. Express **13**, 3653 (2005).
[4] H. Luo, X. Wang, Z. Lio, T. Wang and R. Gong, JEES. **10**, 186 (2010).
[5] P. Dong, J-G. Li and H. W. Yang, J. Modern Opt. **57**, 2137 (2010).
[6] Z. Liu, N. Fang, T-J. Yen and X. Zhang, Appl. Phys. Lett. **83**, 5184 (2003).
[7] D. Schurig and D. R. Smith, Appl. Phys. Lett. **82**, 2215 (2003).
[8] I. V. Shadrivov, A. A. Zharov and Y. S. Kivshar, Appl. Phys. Lett. **83**, 2713 (2003).
[9] D-K. Qing and G. Chen, Appl. Phys. Lett. **84**, 669 (2004).
[10] S. A. Taya, M. M. Shabat and H. M. Khalil, Optik **120**, 504 (2009).
[11] C-H. Lee and J. Lee, Opt. Eng. **51**, 084601 (2012).
[12] R. W. Wood, Phil. Mag. **4**, 396 (1902).
[13] R. W. Wood, Phys. Rev. **48**, 928 (1935).
[14] U. Fano, J. Opt. Soc. Am. **31**, 213 (1941).
[15] W. L. Barnes, A. Dereux, and T. W. Ebbensen, Nature **424**, 824 (2003).
[16] K. L. Tsakmakidis, C. Hermann, A. Klaedtke, C. Jamois and O. Hess, Phys. Review B **73**, 085104 (2006).